Omega-K Algorithm – A Generalization for Highly Squinted Spotlight SAR Imaging with Dechirp-on-Receive

Minh Phuong Nguyen
Institut für Informationsverarbeitung
Leibniz Universität Hannover
Hanover, Germany

Abstract—**Advanced synthetic aperture radar (SAR) systems achieve high spatial resolution by using wide range bandwidth combined with long azimuth illumination time. In order to deal with such sensor parameters, high quality SAR focusing methods and often preprocessing of the raw data are necessary. Omega-K processing is commonly accepted as the ideal solution to the SAR focusing problem. Dechirp-on-receive can be used to reduce the analog bandwidth of SAR raw data. In this paper, a ready for implementation formulation of the Omega-K algorithm for squinted spotlight SAR with dechirp-on-receive is presented. The dechirp-on-receive procedure is analyzed showing that a phase error is induced. A method is presented which compensates this phase error by using a combination of a frequency dependent time shift filter and a constant time shift filter. Therewith, the theoretical achievable resolutions of the focused image reconstructed from both dechirped and chirped input data can be obtained.**

Keywords— **Synthetic Aperture Radar, SAR, squint spotlight, Omega-K, Wavenumber domain, Dechirp-on-Receive**

I. INTRODUCTION

Synthetic aperture radar (SAR) in spotlight mode generates images of the illuminated ground with high azimuthal resolution. In order to enhance the image resolution in range at the same time, pulse bandwidth has to be increased. Often a dechirp-on-receive procedure is then applied to reduce the analog bandwidth of the raw data and the sampling frequency. While the image reconstruction of SAR spotlight mode with a high squint angle requires approximated calculation for many SAR processors, the Omega-K algorithm attains almost the ultimate resolution [1][2]. However, an approach to use the Omega-K algorithm for highly squinted spotlight mode with common dechirp-on-receive has not been described so far.

Dechirp-on-receive systems dechirp a return from a point scatterer using a delayed, inverse replica of the transmitted pulse. The dechirped return from a point scatterer is a sinusoidal signal with a frequency depending on the distance of the point scatterer to the sensor. Range compression is therefore achieved with a Fourier transform. The sinusoidal signal is transformed into a peak located at the corresponding frequency in the frequency domain. The bandwidth of the dechirped signal is much smaller than the bandwidth of the chirped signal. Thus, systems performing dechirp-on-receive usually need lower requirements for their analog-digital-converter in terms of sampling frequency. Dechirping on the one hand reduces the hardware complexity, but on the other hand raises extra effort in the signal processing.

In this paper the dechirp-on-receive procedure is investigated to compare the range compressed output of chirped and dechirped data. The phase error induced by dechirping is derived in closed-form for correction. Furthermore, a ready for implementation formulation of the Omega-K algorithm to deal with both chirped and dechirped data from highly squinted spotlight SAR imaging is presented.

In the following, the Omega-K algorithm for squinted geometry is first described. Afterwards, the processing of chirped and dechirped data are explained. Section V presents the results showing that the theoretical achievable resolution is preserved in both cases.

II. OMEGA-K ALGORITHM FOR SQUINTED SAR

The SAR geometry is shown in Fig. 1. While the platform moves with a constant velocity v along the x-axis, the radar illuminates the ground within $x \in [-L/2, L/2]$. All scatterers can be thought to lie on a conceptual x-z plane, where the z-axis is orthogonal to the x-axis [1].

For the derivation of the proposed generalized Omega-K algorithm, which follows the original paper [1], the range compressed data $d(x, z = 0, t)$ recorded along the platform trajectory at $z = 0$ is considered. The algorithm works with the two-dimensional Fourier transform $D(k_x, z = 0, \omega)$ of the data:

$$d(x, z = 0, t) = \frac{1}{(2\pi)^2} \int_{-\infty}^{\infty} \int_{-\infty}^{\infty} D(k_x, z = 0, \omega) \cdot e^{j(\omega t + k_x x)} d\omega dk_x, \quad (1)$$

where ω is the angular frequency and k_x the azimuthal wavenumber. The origin of the time is placed when recording starts, the measured field $d(x, z = 0, t)$ is considered to be produced by the sources exploding at a time $t = -t_0$. From the measured wave field the map of the sources at depth z can be reconstructed by back-propagation

$$d(x, z, t = -t_0) = \frac{1}{(2\pi)^2} \int_{-\infty}^{\infty} \int_{-\infty}^{\infty} D(k_x, z = 0, \omega) \cdot e^{j(-\omega t_0 + k_x x)} e^{j k_z z} d\omega dk_x. \quad (2)$$

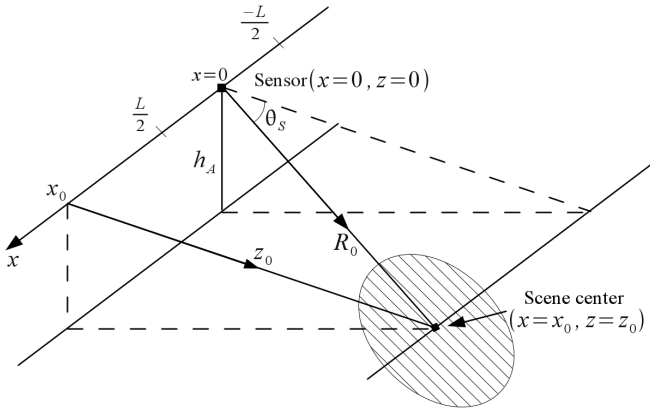In (2) the term $e^{j k_z z}$ takes the spatial shift in z-direction

137

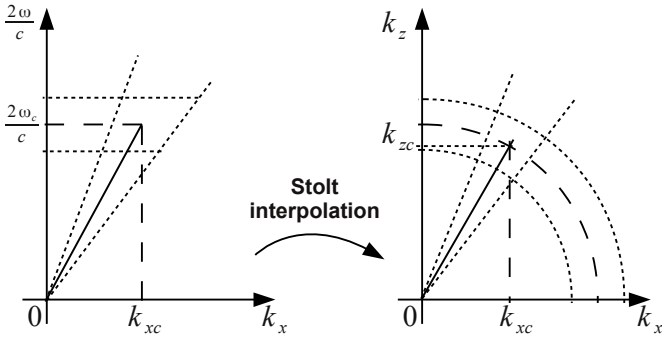Fig. 1: SAR geometry in squinted spotlight mode

Fig. 2: Change of variables $k_z = \sqrt{\left(\frac{2\omega}{c}\right)^2 - k_x^2}$

into account, where k_z is the range wavenumber. In order to solve the integral in equation (2), a change of variables from ω to k_z is needed. The Stolt interpolation, defined by $\omega = \frac{c}{2}\sqrt{k_x^2 + k_z^2}$, gives

$$d(x,\,z,\,-t_0) = \frac{1}{(2\pi)^2} \int_{-\infty}^{\infty} \int_{-\infty}^{\infty} D\left(k_x,\,z=0,\,\frac{c}{2}\sqrt{k_x^2+k_z^2}\right)$$
$$\cdot\, e^{-j\frac{ct_0}{2}\sqrt{k_x^2+k_z^2}} e^{j(k_x x + k_z z)}$$
$$\cdot\, \frac{c|k_z|}{2\sqrt{k_x^2+k_z^2}} dk_z dk_x. \tag{3}$$

The spectrum $D(k_x,\,z=0,\,\omega)$ is band-limited and centered at the carrier circular frequency ω_c in range. In azimuth, $D(k_x,\,z=0,\,\omega)$ is band-limited and centered at a center wavenumber k_{xc}. The squint angle evokes a Doppler shift in azimuth, which becomes apparent at the nonzero center wavenumber k_{xc}, see Fig. 2. After Stolt interpolation, the spectrum $D\left(k_x,\,z=0,\,\frac{c}{2}\sqrt{k_x^2+k_z^2}\right)$ is band-limited and centered at k_{zc}. To facilitate the integral evaluation, variable substitutions $k_x = k'_x + k_{xc}$, $k_z = k'_z + k_{zc}$ are done and yield

$$d(x,\,z,\,-t_0) = \frac{1}{(2\pi)^2} \int_{-\infty}^{\infty} \int_{-\infty}^{\infty} D\left(k_x,\,z=0,\,\frac{c}{2}\sqrt{k_x^2+k_z^2}\right)$$
$$\cdot\, e^{-j\frac{ct_0}{2}\sqrt{k_x^2+k_z^2}} e^{j((k'_x+k_{xc})x+(k'_z+k_{zc})z)}$$
$$\cdot\, \frac{c|k_z|}{2\sqrt{k_x^2+k_z^2}} dk'_z dk'_x. \tag{4}$$

Since only scatterers in the illuminated area around the spot center (x_0, z_0) are expected in $d(x,\,z,\,-t_0)$, the origin of the reconstructed x-z area should be centered at (x_0, z_0). This spatial shift is achieved by variable substitutions $x = x' + x_0$ and $z = z' + z_0$ in equation (4):

$$d(x',\,z',\,-t_0) = \frac{1}{(2\pi)^2} \int_{-\infty}^{\infty} \int_{-\infty}^{\infty} D\left(k_x,\,z=0\,\frac{c}{2}\sqrt{k_x^2+k_z^2}\right)$$
$$\cdot\, e^{j((k'_x+k_{xc})(x'+x_0)+(k'_z+k_{zc})(z'+z_0))}$$
$$\cdot\, e^{-j\frac{ct_0}{2}\sqrt{k_x^2+k_z^2}} \frac{c|k_z|}{2\sqrt{k_x^2+k_z^2}} dk'_z dk'_x \tag{5}$$

$$= \frac{1}{(2\pi)^2} \int_{-\infty}^{\infty} \int_{-\infty}^{\infty} D\left(k_x,\,z=0\,\frac{c}{2}\sqrt{k_x^2+k_z^2}\right)$$
$$\cdot\, e^{j(x'k_{xc}+z'k_{zc})} e^{-j\left(\frac{ct_0}{2}\sqrt{k_x^2+k_z^2} - z_0 k_z - x_0 k_x\right)}$$
$$\cdot\, \frac{c|k_z|}{2\sqrt{k_x^2+k_z^2}} e^{j(x'k'_x + z'k'_z)} dk'_z dk'_x. \tag{6}$$

In equation (6), the phase term $e^{j(x'k_{xc}+z'k_{zc})}$ is independent from the integration variables and describes a two-dimensional (2D) frequency domain shift of k_{xc} in azimuth and k_{zc} in range of $D(k_x,\,z=0,\,\frac{c}{2}\sqrt{k_x^2+k_z^2})$. This shift can be canceled out by using the Fourier transform of the quadrature demodulated, range compressed and Doppler shift corrected SAR data instead of using $D(k_x,\,z=0,\,\omega)$. The term $e^{-j\left(\frac{ct_0}{2}\sqrt{k_x^2+k_z^2} - z_0 k_z - x_0 k_x\right)}$ performs azimuth focusing in 2D frequency domain. The factor $\frac{ct_0}{2} = R_0 = \sqrt{x_0^2 + z_0^2}$ is the distance to the scene center at (x_0, z_0). A point target located at the scene center (x_0, z_0) will be focused and placed at the center of the reconstructed image.

In summary, according to (6) the Omega-K algorithm first performs a 2D Fourier transform on the quadrature demodulated, range compressed and Doppler shift corrected SAR data. The Stolt interpolation then performs the change of variables from the angular frequency ω to k_z. Subsequently, the 2D spectrum is multiplied with the 2D filter

$$H_{mf} = e^{-j\left(\frac{ct_0}{2}\sqrt{k_x^2+k_z^2} - z_0 k_z - x_0 k_x\right)}. \tag{7}$$

The obliquity factor $|k_z|/\sqrt{k_x^2+k_z^2}$ is approximately 1 due to the small relative bandwidth of SAR signals, $k_x^2 \ll k_z^2$ [1]. Finally, the 2D inverse Fourier transform via the double integral $\int\int (\cdot) e^{j(x'k'_x+z'k'_z)} dk'_z dk'_x$ yields the focused data $d(x',\,z',\,-t_0)$, which is the desired SAR image of the illuminated area centered at (x_0, z_0).

III. PROCESSING CHIRPED DATA

In the case of chirped input raw data, range compression is realized by a matched filter in frequency domain, see Fig. 3. Let the transmitted signal $s(t)$ be

$$s(t) = e^{j\pi\gamma t^2} \mathrm{rect}\left\{\frac{t}{T}\right\}, \tag{8}$$

where γ is the positive chirp rate and T the pulse duration. If the return from a point target is received delayed by a time
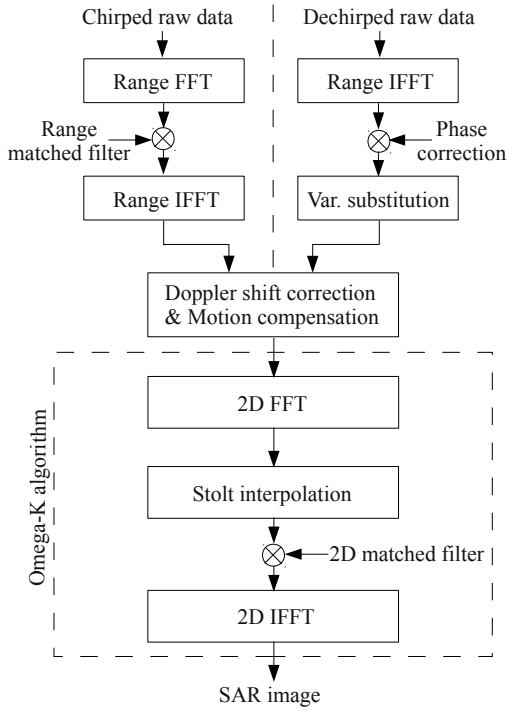
Fig. 3: Block diagram of the generalized algorithm for chirped and dechirped data

t_p, the target's echo can be expressed as

$$s_r(t) = e^{j\pi\gamma(t-t_p)^2}\text{rect}\left\{\frac{t-t_p}{T}\right\}. \qquad (9)$$

The matched filter $h(t)$ is given by

$$h(t) = s^*(-t) = e^{-j\pi\gamma t^2}\text{rect}\left\{\frac{t}{T}\right\}. \qquad (10)$$

If we want to map a target at the scene center with a delay of t_0 to the center of the compressed signal, the results of range compression with frequency domain matched filter is given as

$$s_p(t) = |\gamma|T\text{sinc}\{\pi\gamma T(t-(t_p-t_0))\}. \qquad (11)$$

The mathematical derivation of (11) is analog to the analysis in [3]. After range compression, a Doppler shift correction and if necessary a motion compensation are carried out. The data is then fed into the Omega-K algorithm, see. Fig. 3.

IV. PROCESSING DECHIRPED DATA

In the case of dechirped input data, the dechirped signal $s_d(t)$ can be described by

$$s_d(t) = s_r(t) \cdot s_{ref}(t)$$
$$= e^{j\pi\gamma(t-t_p)^2}\text{rect}\left\{\frac{t-t_p}{T}\right\} e^{-j\pi\gamma(t-t_0)^2}\text{rect}\left\{\frac{t-t_0}{T_{ext}}\right\}$$
$$= e^{-j2\pi\gamma(t_p-t_0)t}e^{j\pi\gamma(t_p^2-t_0^2)}\text{rect}\left\{\frac{t-t_p}{T}\right\}, \qquad (12)$$
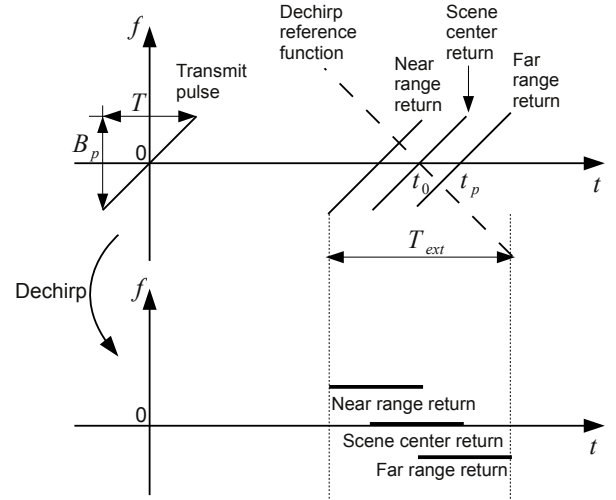

Fig. 4: Dechirp-on-receive procedure for SAR raw data of three targets at different range. Each return is described by its frequency as a function of time.

where $s_{ref}(t) = e^{-j\pi\gamma(t-t_0)^2}\text{rect}\left\{\frac{t-t_0}{T_{ext}}\right\}$ is the dechirp reference function, see Fig. 4. Range compression is achieved with an inverse Fourier transform applied on $s_d(t)$ resulting

$$s_{foc}(f) = T\text{sinc}(\pi T(f-\gamma(t_p-t_0)))$$
$$\cdot e^{j\pi\gamma(t_p^2-t_0^2)}e^{j2\pi(f-\gamma(t_p-t_0))t_p}, \qquad (13)$$

where t_p-t_0 is the delay time difference between a point target and the scene center. For the linear frequency modulation of the range chirp signal, the substitution $t = f/\gamma$ can be applied, resulting in

$$s_{foc}(t) = T\text{sinc}(\pi T\gamma(t-(t_p-t_0)))$$
$$\cdot e^{j\pi\gamma(t_p^2-t_0^2)}e^{j2\pi\gamma(t-(t_p-t_0))t_p}. \qquad (14)$$

Comparing the focused range signal in (14) and equation (11), it is evident that the phase term is an undesirable phase error as a consequence of dechirping. This phase error is absent in situations that use matched filter processing to accomplish range compression. However, this phase error is systematic and can be fully compensated by applying proper filters on $s_{foc}(f)$. The first part of the phase error in (13) can be rearranged as

$$e^{j\pi\gamma(t_p^2-t_0^2)} = e^{j2\pi\gamma t_0(t_p-t_0)}e^{j\pi\gamma(t_p-t_0)^2}$$
$$= e^{j2\pi t_0 f_p} \cdot e^{j\frac{\pi}{\gamma}f_p^2}|_{f_p=\gamma(t_p-t_0)}. \qquad (15)$$

Thus, to compensate the phase error, the signal $s_{foc}(f)$ needs to be multiplied with

$$H_{cor}(f) = e^{-j2\pi t_0 f} \cdot e^{-j\frac{\pi}{\gamma}f^2}. \qquad (16)$$

This correction is done for every $f = f_p$ of every picture element to correct the phase error induced by any target p. $H_{cor}(f)$ consists of a linear term $H_{lin}(f) = e^{-j2\pi t_0 f}$ and a quadratic term $H_{RVP}(f) = e^{-j\frac{\pi}{\gamma}f^2}$. The quadratic term
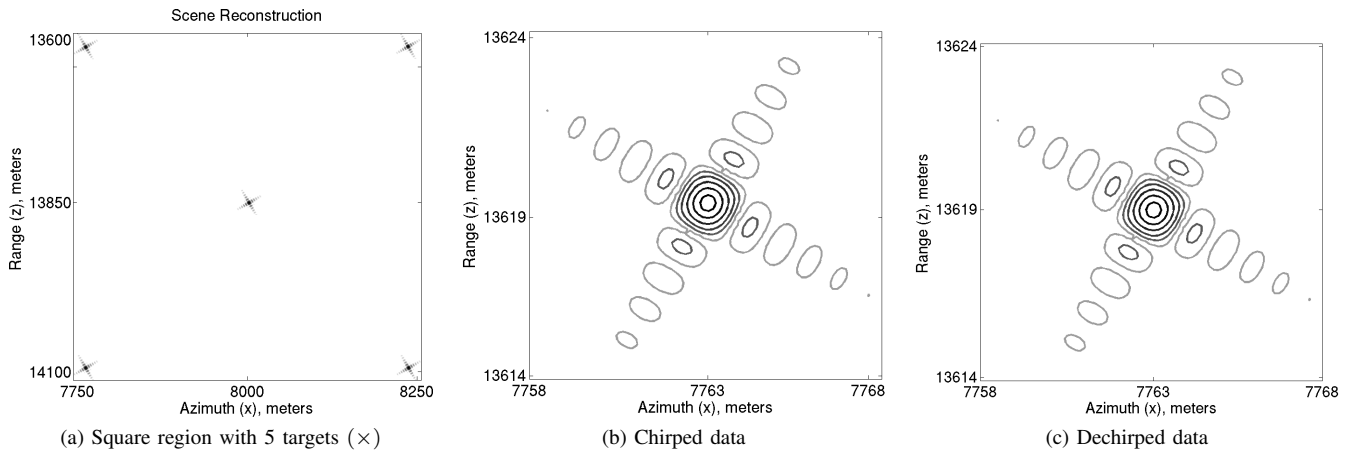
Fig. 5: Simulation results. In (b)(c) top left point target is zoomed.

is known as range deskew and is described in [2] for non-squinted SAR systems.

It has to be emphasized that only by applying both $H_{lin}(f)$ and $H_{RVP}(f)$ together, the phase error $e^{j\pi\gamma(t_p^2 - t_0^2)}$ can be fully compensated. Furthermore, by multiplication with $H_{cor}(f)$ for every $f = f_p$, the second phase error $e^{j2\pi(f-\gamma(t_p-t_0))t_p} = e^{j2\pi\gamma(f-f_p)t_p}$ in (13) is automatically compensated to 1. The phase error compensation applied on (13) results $s_{cor}(f)$

$$
\begin{aligned}
s_{cor}(f) &= s_{foc}(f) \cdot H_{cor}(f) \\
&= T\mathrm{sinc}(\pi T(f - \gamma(t_p - t_0))).
\end{aligned}
\tag{17}
$$

Finally, the substitution $t = f/\gamma$ yields the desired time signal

$$
s_{cor}(t) = T\mathrm{sinc}(\pi\gamma T(t - (t_p - t_0))).
\tag{18}
$$

Comparison between (11) and the range compressed, phase error compensated signal in (18) now shows that both results are identical except for a constant factor, which has no relevance since normalization is carried out in practice.

V. RESULTS

Fig. 5 presents simulation results with parameters shown in Table I. Five targets are distributed in a square region of the size (500m × 500m). With a reference range $R_0 = 16$ km and a squint angle $\theta_s = 30°$, the scene center is located at ($x_0 = 8$km, $z_0 = 13.856$km). SAR raw data from the five targets were simulated and submitted to the two processing chains showed in the flow chart in Fig. 3. Comparing the results of the image reconstruction from chirped and dechirped data, we can see that in both cases the theoretical achievable resolutions in range and azimuth are attained. In contrast to a recent paper [4], this approach preserves the geometry of the 2D point target response.

The focusing results remain good for squint angles up to at least 62°.

TABLE I: Simulation parameters

Carrier frequency f_c	10 GHz
Pulse bandwidth B_p	150 MHz
Pulse duration T	6 μs
Sample frequency	180 MHz
Platform velocity v	100 m/s
Synthetic aperture length	300 m
Pulse repetition frequency	400 Hz

VI. CONCLUSION

A generalized and ready for implementation Omega-K algorithm for squinted SAR imaging is presented in this paper. The advantage of the presented work is that through a post-processing step after range compression in case of dechirped data, the Omega-K algorithm kernel is the same for both chirped and dechirped data. The SAR image reconstruction is optimal for both chirped and dechirped raw data. However, motion errors have not been considered in this study. Since precise compensation of motion errors in most airborne SAR systems is crucial for the focusing results [5], further work will address this issue.

REFERENCES

[1] C. Cafforio, C. Prati and F. Rocca, SAR *data focusing using seismic migration techniques*, IEEE Transaction on Aerospace and Electronics Sytems, pp. 194-207, March 1991.

[2] W. G. Carrara, R.S. Goodman and R. M. Majewski, *Spotlight synthetic aperture radar*, Artech House, Boston, 1995.

[3] I. G. Cumming and F. H. Wong, *Digital processing of synthetic aperture radar data, Chapter 3.3.3*, Artech House, Boston, 2005.

[4] An Daoxiang, Huang Xiaotao et al., *A modified range migration algorithm for airborne squint-mode spotlight* SAR *imaging*, Radar Conference, 2010 IEEE, pp. 1183-1886, 10-14 May 2010

[5] A. Reigber, A. Moreira et al., *Extended wavenumber-domain synthetic aperture radar focusing with integrated motion compensation*, IEE Proc.-Radar Sonar Navig., Vol. 153, No. 3, June 2006